A tunable diode laser absorption spectrometer for formaldehyde atmospheric measurements validated by simulation chamber instrumentation

Valéry Catoire, François Bernard, Y. Mébarki, Abdelwahid Mellouki, Grégory Eyglunent, Véronique Daële, Claude Robert

A tunable diode laser absorption spectrometer for formaldehyde atmospheric measurements validated by simulation chamber instrumentation

V. Catoire[1]*, F. Bernard[2], Y. Mébarki[1], A. Mellouki[2], G. Eyglunent[2], V. Daële[2], C. Robert[1]

1. Laboratoire de Physique et Chimie de l'Environnement et de l'Espace (LPC2E), CNRS-Université d'Orléans (UMR 6115), Observatoire des Sciences de l'Univers en région Centre (OSUC) , *3A Avenue de la Recherche Scientifique, 45071 Orléans Cedex 2, France*

2. Institut de Combustion, Aérothermique, Réactivité et Environnement (ICARE), CNRS (UPR 3021), Observatoire des Sciences de l'Univers en région Centre (OSUC), *1C Avenue de la Recherche Scientifique, 45071 Orléans Cedex 2, France*

* Corresponding author. Email: Valery.Catoire@cnrs-orleans.fr

Abstract

A tunable diode laser absorption spectrometer (TDLAS) for formaldehyde atmospheric measurements has been set up and validated through comparison experiments with a Fourier transform infrared spectrometer (FTIR) in a simulation chamber. Formaldehyde was generated *in situ* in the chamber from reaction of ethene with ozone. Three HCHO ro-vibrational line intensities (at 2909.71, 2912.09 and 2914.46 cm^{-1}) possibly used by TDLAS were calibrated by FTIR spectra simultaneously recorded in the 1600-3200 cm^{-1} domain during ethene ozonolysis, enabling the on-line deduction of the varying concentration for HCHO in formation. The experimental line intensities values inferred confirmed the calculated ones from the updated HITRAN database (Rothman et al., 2009, based on Perrin et al., 2009). In addition, the feasibility of stratospheric *in situ* HCHO measurements using the 2912.09 cm^{-1} line was demonstrated. The TDLAS performances were also assessed, leading to a 2σ detection limit of 88 ppt in volume mixing ratio with a response time of 60 s at 30 Torr and 294 K for 112 m optical path. As part of this work, the room-temperature rate

constant of this reaction and the HCHO formation yield were found to be in excellent agreement with the compiled literature data.

Keywords: formaldehyde, ethene ozonolysis, *in situ* measurements, stratosphere, simulation chamber, infrared tunable diode laser absorption spectrometry (TDLAS), Fourier Transform Infrared spectrometry (FTIR).

1 Introduction

Formaldehyde plays a key role in the odd hydrogen family (HO_x = OH + HO_2) chemistry, with its subsequent involvement in HO_2 production (Seinfeld and Pandis, 2006). The largest sources of tropospheric HCHO come from the oxidation of methane (CH_4) and other non-methane volatile organic compounds (VOCs), which have both natural and anthropogenic origins (Anderson et al., 1996). Biomass burning, incomplete combustion, emissions from industries and vegetation represent the main direct emission sources (Carlier et al., 1986; Lee et al., 1998). The main loss processes include photolysis by ultraviolet (UV) radiation and oxidation by OH radicals. Formaldehyde removal can also take place through dry deposition, heterogeneous loss on aerosol particles (Tie et al., 2001), cloud chemistry and precipitation scavenging (e.g., Lelieveld and Crutzen, 1990; Heikes, 1992). HCHO has its greatest mixing ratio in the boundary layer, near its emission sources. Its abundance decreases with altitude up to the upper troposphere, where it can reach values as low as a few tens of ppt in volume mixing ratios (Dufour et al., 2009). The lifetime of formaldehyde regarding the major chemical and physical removal pathways is of the order of a few hours in the troposphere (Possanzini et al., 2002). In the upper troposphere, HCHO is found to be a relevant indicator for testing the presence of additional HO_x precursor species possibly moved upward by convective transport (Crawford et al., 1999). In the stratosphere, the abundance of HCHO

increases with altitude, mainly as a result of the oxidation of methane by OH and $O(^1D)$, resulting in a "C-shaped" vertical profile from the troposphere to the stratosphere (Barth et al., 2007).

Formaldehyde concentrations have never been measured *in situ* in the stratosphere. Up to now, only three remote vertically resolved satellite measurements of HCHO have been reported, one by SMR (Sub-Millimeter Radiometer) aboard Odin satellite (Ricaud et al., 2007) in the upper stratosphere (> 35 km altitude), and the other ones by MIPAS (Michelson Interferometer for Passive Atmospheric Sounding) aboard Envisat (Steck et al., 2008) and by FTS (Fourier Transform Spectrometer) aboard ACE-SCISAT (Coheur et al., 2007; Dufour et al., 2009). Whereas the MIPAS measurements are performed using several spectral micro-windows in the 5.7 μm region (i.e., the ν_2 band centred at 1746 cm^{-1}), the FTS measurements use the 3.6 μm region (i.e., around 2600-3100 cm^{-1}). Formaldehyde indeed shows strong ν_1 and ν_5 fundamental vibration bands centred at 2782 and 2844 cm^{-1}, respectively.

TDLAS (Tunable Diode Laser Absorption Spectrometry) measurements of HCHO in the upper troposphere aboard aircrafts have been pioneered by Fried and co-workers using the 2831.64 cm^{-1} ro-vibrational line of the ν_5 band (Fried et al., 2008, and references therein). SPIRALE (SPectroscopie Infra Rouge par Absorption de Lasers Embarqués) is a balloon-borne instrument using the TDLAS method for simultaneous *in situ* measurements of numerous trace gases (e.g., O_3, CH_4, CO, OCS, N_2O, HNO_3, NO_2, NO, HCl, COF_2, H_2O_2) with a high vertical resolution (~ 5 m) (Moreau et al., 2005) in the upper troposphere and the stratosphere. SPIRALE measurements have been used for dynamics and chemistry studies (see e.g., Berthet et al., 2006; Huret et al., 2006; Berthet et al., 2007; Müller et al., 2007; Pirre et al., 2008; Mébarki et al., 2010), as well as for validation of stratospheric species abundances measured by satellite instruments such as Envisat MIPAS and GOMOS (Global Ozone Measurement by the Occultation of Stars), ACE-SCISAT FTS and Odin SMR (see e.g., Wang et al., 2007; Renard et al., 2008; Strong et al., 2008; Jégou et al., 2008). One of the six SPIRALE lasers can now operate in the R-branch most intense lines of the ν_5 band, with three emission modes included between 2909 and 2915 cm^{-1}, which opens possibility for field measurements.

Several spectroscopic studies have reported line parameters for the ν_5 band, but with intensities in disagreement with each other by up to a factor of three (Rothman at al., 2005, Herndon et al., 2005, Perrin et al., 2006, Perrin et al., 2009). The study of Perrin et al. (2009)

recently identified the reasons of the discrepancies and has been included into the new HITRAN database (Rothman at al., 2009). The existence of numerous overtones and combination bands has sometimes led to inconsistencies in blended or degenerate doublet lines. This study derived a consistent set of line intensity parameters for both the 3.6 and 5.7 μm bands, based on some FTIR (Fourier Transform Infra Red) lines measurements covering the whole domain (1600–3200 cm^{-1}) and on theoretical spectroscopy calculations. However, this study is the first one delivering consistent values, which needs confirmation, all the more so as two of the three line intensities in the range 2909-2915 cm^{-1} were not directly measured.

The first goal of the present study is to determine the absolute intensity of these specific lines in order to allow for deriving reliable stratospheric HCHO concentrations using airborne or balloon-borne instruments such as SPIRALE. Our line calibrations were performed using FTIR spectra covering the whole region (around 1600-3200 cm^{-1}) simultaneously recorded in an atmospheric simulation chamber, and hence with consistent values between both bands. The well-known chemical reaction system of ethene ozonolysis was used as source of formaldehyde. Given this compound is sticky and polymerizable, its concentration determination is rather challenging (Gratien et al., 2007; Brauers et al., 2007; Perrin et al., 2009). In the present study, HCHO was thus produced *in situ*, which has the great advantage to lead to low and so, accurate concentrations, since no polymerization and wall adsorption was expected. The second goal of the study is to evaluate the interest of implementing TDLAS instrumentation in the simulation chamber of ICARE-Orléans. The conventional methods currently used for laboratory measurements of formaldehyde are limited in detection limit (> 50 ppt in volume mixing ratio units) and/or in measurement frequency (> 1 min) (Hak et al., 2005; Wisthaler et al., 2008; Hottle et al., 2009; Jobson and McCoskey, 2010). TDLAS method is expected to be at least as sensitive, and is known to perform rapid on-line measurements (in a few seconds), which is the main reason for its use aboard mobile instruments such as airborne or balloon-borne spectrometers. In the case of static measurements performed in laboratory simulation chambers, the very short response time should allow for lowering the detection limit and improving the accuracy of the kinetics and mechanistic studies. The well-established reaction of ethene with ozone has been used in the present work to test the TDLAS potentiality with respect to the already existing chamber instrumentation.

2 Experimental

2.1 The Atmospheric Simulation Chamber

Experiments were carried out in the 7300 L ICARE indoor atmospheric simulation made of Fluorene-Ethene-Propene (FEP) foil (DuPont) with a parallelepiped shape. The experiments were performed at 294±1 K in dry purified air (relative humidity, RH < 2%). The chamber was operated at ~0.08 Torr above the atmospheric pressure in order to avoid external contamination and to compensate the sampling flows of the various instruments connected to the chamber. This was achieved during the experiments by continuously adding 5 to 20 L min^{-1} of purified air. Between experiments, the chamber was cleaned by flushing it with purified air at a flow rate of ~100 L min^{-1} for at least 12 h. A fan made of Teflon insured homogeneous mixing of the reactant within ~1 min.

Temperature and relative humidity were monitored by a combined sensor (T870 – Series T800, Dostmann electronic) and the differential pressure was measured using an MKS gauge (0-10 Torr range). The chamber is equipped with an *in situ* FTIR spectrometer (Nicolet 5700 Magna) coupled to a White-type multipass cell resulting in an optical path length of 166 m. HgCdTe/B semiconductor was used as detector and cooled with liquid nitrogen at a temperature close to 77 K. The instrument was operated in the mid-IR region, from 4000 to 600 cm^{-1}. The IR spectra were recorded every 4 min 15 s by co-adding 110 interferograms with a resolution of 1 cm^{-1}, using Happ-Genzel apodization. IR spectra acquisition was operated using OMNIC software (OMNIC, Thermo Electron Corporation, version 6.2). Reactants (ethene and ozone) and products were monitored during the course of the reaction and their concentrations were determined using calibrated reference spectra. The chamber is also equipped with gas monitors for ozone (Horiba, APOA-360) and NO, NO_2 and NO_x (Horiba, APNA-360), which enabled to measure the O_3 concentration and any NO_x background during the experiments. Ozone was generated from an electric discharge in an oxygen flow of 2 L min^{-1} capable of fast introduction into the chamber, which enables to reach the desired concentration in few minutes. Known amounts of the C_2H_4 and SF_6 were introduced into the chamber using a calibrated 0.9 L cylinder equipped with two pressure gauges (0-10 Torr and 0-1000 Torr, MKS Baratron). All experiments presented here were conducted in the dark.

Dilution and leak rates were determined before the start of each experiment by monitoring the decay of added amount of SF_6 (190 ppb volume mixing ratio) using the IR band (948 cm^{-1}). This decay rate was found to be in the range (1-4) × 10^{-5} s^{-1} depending on the experimental conditions (added flow during the runs). Ozone was injected before adding ethene, in order to estimate its total loss rate. This one was found to be slightly higher than that of SF_6 (~ 2.6-7.9 × 10^{-5} s^{-1}). Ethene loss rate, determined in independent runs, was found to be similar to that of SF_6. Before each experiment, background concentrations in the chamber were checked systematically and found to be lower than the detection limits (e. g., $[NO_x] < 1$ ppb, $[O_3] < 1$ ppb).

2.2 The Tunable Diode Laser Absorption Spectrometer (TDLAS)

Gas mixture samples from the simulation chamber were continuously collected via a PFA Teflon tube (6 mm o.d.) and passed through the TDLAS multipass absorption cell, with a controlled flow of 3.0 L min^{-1}, using a scroll pump (XDS10 Boc Edwards). It is known that loss of HCHO in the sampling line made of Teflon is not significant (Wert et al., 2002; Herndon et al., 2007). This has been verified by observing no concentration change in the TDLAS cell when the tube length was varied by a factor of two. The pressure cell was around 30 Torr, precisely known (±0.1 Torr) using a 0-100 Torr range gauge (MKS Baratron), and maintained constant by tuning a simple valve located at the cell output, upstream of the pump. This pressure reduction enabled the cell content to be completely renewed in less than 4 s, which allows for high frequency measurements. The low pressure also allows for the trace gas species ro-vibrational lines broadening to be reduced, so that the molecular lines were clearly distinguished and the baseline (i.e. the laser signal without absorption) was easily interpolated, which improves the measurement accuracy and the sensitivity.

The multiple reflection absorption cell used in this work has been already described in detail elsewhere (Robert, 2007). In brief, it consists of three spherical mirrors as in a White cell but its principle is different. It behaves as a multiplier of a Herriott cell from which it inherits the opto-mechanical stability qualities. The Herriott cell and the White cell are two particular cases of this type of cell. The main advantages of this cell are that it is made of standard mirrors, it is easily set up and tuned for adjusting the path length (by rotation of only one mirror), and it is compact, while allowing a great number of reflections and thus a large optical path (potentially more than 280 m). In the configuration used in the present

experiments, the total optical path length was 112.3 m, determined by counting the visible spots of a laser diode (He-Ne) on the mirrors before the measurements. The three mirrors are of equal curvature (with a radius of 2500 mm) and the separation between the opposite ones is 1.08 m. The mirror coating is protecting gold, with an effective reflection coefficient of 98% in the present case, which restricted the path length to the above value. The mirrors are set in the hermetically sealed cell with two windows (ZnSe wedge) for the input/output laser beam passing.

The acquisition and detection systems are from SPIRALE instrument, already described in detail (Moreau et al., 2005) and therefore summarized hereafter. A lead-salt laser diode (Laser Components Instruments Group) produced several pure single mode radiations of typically less than 1 mW power. The three modes selected for the present study emitted in the spectral micro-windows 2909.2-2909.9, 2911.8-2912.2, and 2914.1-2914.8 cm^{-1}, inferred from reference spectra of pure gaseous carbonyl sulphide (OCS) provided by a commercial cylinder. The relative spectral scale is determined by the use of a Fabry–Pérot interferometer, as previously reported (Moreau et al. 2005; Joly et al., 2008). Mode purity was checked by observing that null optical transmission from saturated lines of concentrated OCS contained in an external small cell and the laser switching-off give equal electrical signals. Cooling the laser at 96.6-97.1 K using liquid nitrogen and applying a current of typically 305-310 mA enabled emission at the selected wavenumber regions. The spectral windows were swept by applying an asymmetric saw-tooth ramp of about 30 mA at ~200 Hz frequency around the current value and averaging every 1.1 s. Each spectrum is composed of 1024 points, which gives very high spectral resolution (~ 4-7 × 10^{-4} cm^{-1}) depending on the micro-window (~0.4-0.7 cm^{-1}) swept by the laser. The laser beam was directed through the multipass cell where it was selectively absorbed by the HCHO spectral features. The output beam was directed onto a liquid-N_2 cooled HgCdTe detector.

3 Results and discussion

Formaldehyde has been generated in the chamber under two types of experimental conditions, corresponding to two different concentration levels of C_2H_4 and O_3: one at higher concentration in order to calibrate the TDLAS instrument using FTIR spectroscopy measurement, and another one at lower concentration to intercompare TDLAS and FTIR performances. This formaldehyde production mean has been earlier used by different groups

for the calibration of instruments working at atmospheric concentration levels of formaldehyde (e.g. Brauers et al., 2007). Both sets of experiments were conducted without adding OH radicals scavenger to the reactants mixture (that could be generated during the ozonolysis of ethene), which implies that formaldehyde could also be produced through the reaction of OH with ethene (Paulson et al., 1999; Rickard et al., 1999; Mihelcic et al., 1999; Fenske et al., 2000; Kroll et al., 2001).

3.1 Rate constant of the reaction of ozone with ethene

Prior to TDLAS calibration, a check of the chemical system used to generate formaldehyde was performed by deriving the rate constant value for the ethene ozonolysis reaction under pseudo-first order conditions. The measurements were conducted at 760±1 Torr and 294±1 K. One typical initial set of C_2H_4 and O_3 volume mixing ratios was 4.5±0.3 ppm and 465.0±0.1 ppb, respectively. Figure 1 shows the plot of ozone consumption versus reaction time in the absence and presence of C_2H_4 for these initial conditions. The reaction rate constant derived from this run is $k = (1.55\pm0.11) \times 10^{-18}$ cm^3 molecule^{-1} s^{-1}, which is in excellent agreement with the recommended value $k = (1.6\pm0.2) \times 10^{-18}$ cm^3 molecule^{-1} s^{-1} (Atkinson et al., 2006), indicating that the consumption of O_3 in our experimental system was not affected by any noticeable side reactions.

3.2 Validation of the formaldehyde FTIR spectrum recorded in the Euphore atmospheric simulation chamber

The reaction of ozone with ethene is known to produce formaldehyde with a yield near unity (Horie and Moortgat, 1998; Neeb et al., 1998; Brauers et al., 2007; Wegener et al., 2007). In addition, OH radicals are also produced, with a yield of ~ 0.16 (Atkinson et al., 2006). The OH radicals formed could react with both ethene and formaldehyde. However, considering the concentrations of O_3 and ethene used in this first experiment and the room-temperature reaction rate constant of OH with HCHO ($k = 8.5 \times 10^{-12}$ cm^3 molecule^{-1} s^{-1}) and with C_2H_4 ($k = 7.9 \times 10^{-12}$ cm^3 molecule^{-1} s^{-1}) (Atkinson et al., 2006), it can be concluded that the OH radicals react essentially with ethene. Hence, the observed HCHO resulted from the reactions of ethene with both OH and O_3.

During the experiments, HCHO concentrations were derived using a scaled reference spectrum recorded between 4000 and 400 cm^{-1} at the Euphore facilities (EUPHORE FTIR

References Database). This spectrum, displayed in Fig. 2, has been recorded for a HCHO mixing ratio of 892.4 ppb at T = 296.5 K and P =1004.5 mbar, i.e. 2.21×10^{13} molecule cm^{-3}, obtained with 553.4 m path length and a resolution of 1 cm^{-1}. 1σ-precision has been attributed to the FTIR HCHO measurement, resulting in 6% uncertainty on the measured concentration.

The calibration of the Euphore IR spectrum has been obtained with only one injection of paraformaldehyde. Therefore, Integrated Band Intensities (IBIs) have been calculated in order to ensure the reliability of this spectrum. The IBIs have been defined in the ranges 1660-1820 and 2600-3100 cm^{-1} and compared to the existing literature data. In a given spectral region, an IBI is determined using Beer-Lambert law, as follows:

$$A = \sigma \times L \times c \quad (1)$$

where A is the IR absorbance (base e) for a given wavenumber $\tilde{\nu}$, σ is the absorption cross section (in cm^2 $molecule^{-1}$), L is the absorption path length (in m) and C is the HCHO concentration (in molecule cm^{-3}). By integration on the spectral region,

$$\int A \times d\tilde{\nu} = \int \sigma \times L \times C \times d\tilde{\nu} \quad (2)$$

The IBI can be deduced as

$$IBI = \int \sigma \times d\tilde{\nu} \quad (3)$$

The values obtained using the Euphore spectrum are in excellent agreement with those reported in the literature, as shown in Table 1. The Euphore values, $(1.265 \pm 0.063) \times 10^{-17}$ cm $molecule^{-1}$ at 1660-1820 cm^{-1} and $(2.830 \pm 0.141) \times 10^{-17}$ cm $molecule^{-1}$ at 2600-3100 cm^{-1}, match within 1% the average of the previous values, $(1.263 \pm 0.030) \times 10^{-17}$ cm $molecule^{-1}$ and $(2.805 \pm 0.087) \times 10^{-17}$ cm $molecule^{-1}$, respectively. Moreover, the ratio 2.24 between the 2600-3100 and 1660-1820 cm^{-1} Euphore IBIs is in excellent agreement with the previous determined ratios 2.21-2.25 (Perrin et al., 2009). Therefore, we used this Euphore IR spectrum to derive the absolute concentrations of formaldehyde $[HCHO]_{ICARE}$ (in molecule cm^{-3}) obtained at the ICARE chamber using the formula:

$$[HCHO]_{ICARE} = [HCHO]_{Euphore} \times \frac{L_{Euphore}}{L_{ICARE}} \times \frac{T_{ICARE}}{T_{Euphore}} \times \frac{P_{Euphore}}{P_{ICARE}} \quad (4)$$

where $[HCHO]_{Euphore}$ is the HCHO concentration of the calibrated spectra (in molecule cm^{-3}), *L* the optical path lengths (in m), *T* the temperatures (in K) and *P* the pressures (in Torr) of the considered chambers. These results led to consistency between the concentrations of HCHO

derived from the bands centred at 1746 cm^{-1} (i.e., the 1660-1820 cm^{-1} region) and at 2800 cm^{-1} (i.e., the 2600-3100 cm^{-1} region), which are found equal within uncertainties (1%) and very well correlated (R^2 = 0.9937), as shown in Fig. 3.

3.3 Formaldehyde formation yield deduced from FTIR spectrometry

Both FTIR bands have been used to quantify the formation yield of formaldehyde from the runs conducted in the first experimental conditions (e.g., with initial volume mixing ratios: $[C_2H_4]_0$ = 4.5 ppm and $[O_3]_0$ = 465 ppb). Figure 4 shows a linear regression of the plot of HCHO concentration with respect to ozone consumption at the first stage of the reaction, which leads to a formation yield of (0.96±0.04; r^2 = 0.9884) and (0.90±0.03; r^2 = 0.9961) using the 1746 and 2800 cm^{-1} centred bands, respectively, and so, to a mean value of 0.93±0.05. This result is in good agreement with the previous published data, i.e. 0.77-1.00 (Horie and Moortgat, 1998; Neeb et al., 1998; Brauers et al., 2007; Wegener et al., 2007) and thus gives great confidence in the reliability of the HCHO concentration measured by the FTIR apparatus. Moreover, the absence of formaldehyde polymerization due to the *in situ* generation of HCHO at very low partial pressure (< 0.001 hPa) is validated, in agreement with Gratien et al. (2007).

3.4 Calibration of the ro-vibrational line intensities measured by TDLAS by FTIR spectrometry

The absorption cross section at a given wavenumber $\tilde{\nu}_0$ can be expressed as:

$$\sigma(\tilde{\nu}_0) = S(\tilde{\nu}_0).\, g\left(\tilde{\nu} - \tilde{\nu}_0\right) \tag{5}$$

where $S(\tilde{\nu}_0)$ is the ro-vibrational line intensity (in cm $molecule^{-1}$) and $g(\tilde{\nu} - \tilde{\nu}_0)$ is the normalized absorption profile (in cm). The calibration of the line intensities is based on the Beer-Lambert law:

$$S(\tilde{\nu}_0) = \frac{A}{C.g\left(\tilde{\nu} - \tilde{\nu}_0\right).L} \tag{6}$$

where C is the HCHO concentration (in molecule cm^{-3}), A is the absorbance (in base e) and L is the path length (in cm). The principle of the retrieval is to fit the experimental absorbance A to the synthetic one, $S(\tilde{\nu}_0).C.\, g(\tilde{\nu} - \tilde{\nu}_0).L$, by adjusting the line intensity $S(\tilde{\nu}_0)$. A linear least-square algorithm (of Levenberg-Marquardt) was used for minimizing the difference between these experimental and synthetic absorbances. The HCHO concentration C is known from the

FTIR simultaneous measurements. This calibration was performed at high HCHO concentrations, corresponding to volume mixing ratios above 250 ppb, to maximise the signal-to-noise ratio and therefore the precision. The profile $g(\tilde{\nu}-\tilde{\nu}_0)$ is the convolution of the HCHO molecular Voigt profile, including the air-collisional broadening and the Doppler broadening half-widths, with the laser linewidth determined at lower pressure (~ 6 hPa) where its magnitude is not negligible compared to the air-collisional broadening. The air-broadening half-widths and the line positions (the central wavenumber $\tilde{\nu}_0$) were taken from Perrin et al. study (2009), in order to realize direct comparisons with this study and because there was no means to measure these parameters in our present experiments. Moreover, since our experiments were all performed at constant temperature, 294±1 K, the temperature dependencies of the air-broadening coefficients and of the line intensities were not taken into account. Figure 5 shows an example of experimental and simulated transmission (*T*) spectra from which the absorbance ($A = -\ln T$) can be deduced, and the associated residual, i.e. the difference between the experimental and the synthetic spectra.

All the results are gathered in Table 2 and compared to the previous studies. Given our experimental pressure conditions (leading to line broadening) and the TDLAS resolution, ro-vibrational lines positioned closer than 10^{-2} cm^{-1} are undistinguished in our experiments. Therefore, the comparison is made with the sum of the individual line intensities of the other studies within this limit. The overall uncertainties have been evaluated. The main systematic error originates from the laser linewidth determination (9%). The precision includes the experimental scatter (1.3% at 1σ level for seven determinations) and the precision on the fit (2%, 1σ). Using the error propagation method (i.e. the square root of the quadratic sum of all errors) leads to an estimated overall uncertainty of about 10%. The agreement is good with the calculated values Perrin et al. (2009) for the lines at 2909.71 cm^{-1} (within 13%) and 2914.46 cm^{-1} (within 9%), and very good (within 4%) for the 2912.09 cm^{-1} line, taking into account the 7% uncertainty of the later. The agreement is also very good at 2914.46 cm^{-1} (within 3.4%) if the experimental value obtained in this study is taken ($5.91\pm0.3 \times 10^{-20}$ cm $molecule^{-1}$; Jacquemart, 2009). In contrast, this is clearly not the case for the previous HITRAN 2004 database (Rothman et al., 2005), with over evaluations ranging from about 50 to 150%. We then confirm the validity of the line intensities calculated by Perrin et al. (2009) included in the new HITRAN database (Rothman et al., 2009). Thus, the use of FTIR bands, consistent each other between both spectral domains (1660-1820 and 2600-3100 cm^{-1}) and in

agreement with the study by Perrin et al. (2009), leads to sensible and reliable results for the particular lines studied here. The interest of using one of these lines for *in situ* stratospheric measurements is developed in Section 3.6, compared with the other lines in the 3.6 μm (2600-3100 cm^{-1}) spectral region.

3.5 Performances of the TDLAS instrument

The other goal of the study was to assess the performances of the TDLAS instrument, with a view of completing the atmospheric simulation chamber instrumentation. A second set of experiments of ethene ozonolysis at 760±1 Torr and 294±1 K has been performed to this end, with initial much lower O_3 and C_2H_4 volume mixing ratios (e.g., 219.0±0.1 ppb and 681±30 ppb, respectively) giving rise to lower production levels of formaldehyde (< 25 ppb in 1.5 h reaction time). Only the 2800 cm^{-1} centred band was used for HCHO quantification by FTIR due to a better sensitivity than the 1746 cm^{-1} centred band. Using one of the TDLAS lines studied reported in the above section, we could simultaneously follow the HCHO formation with a high frequency (each 1.1 s; see section 2.2), as illustrated in Fig. 6 for the above quoted initial mixing ratios. Of course, due to the calibration of the TDLAS by the FTIR spectrometer, the results of both techniques are in agreement. However, what is particularly noticeable is the greater data number with less experimental scatter for TDLAS than for FTIR, as shown with 1σ error bars labelled on each measurement point for both setups in Fig. 6. The 1σ precision for TDLAS with 4 s averaging (the time for cell replenishment by the gases) for 112.3 m path length is 170 ppt HCHO at 40 hPa (30 Torr), whereas the 1σ precision for FTIR is ~2.4 ppb (166 m path length) in 255 s response time. This TDLAS precision leads to a 2σ detection limit of 88 ppt in 60 s acquisition time (the sensitivity of the technique increased as the square root of the collection time). So, the TDLAS short response time allows for lowering the detection limit of the reaction products, e.g. HCHO in the present study, and thus improves the accuracy of reaction mechanism studies (e.g., the branching ratios of multichannel reactions). These performances are similar as those from another TDLAS (Fried et al., 2008), as shown in Table 3, and should even be improved to a detection limit of 35 ppt in 60 s if the path length would be increased to 280 m, which seems possible with mirrors of better quality (reflectivity > 99%) than the current ones. In contrast, Fried et al. (2008) used a multipass absorption cell that does not allow for reaching a so long optical path, and the sensitivity and accuracy of their HCHO measurements

are primarily due to the removing of H_2O (which generates spectroscopic interferences) and to the calibration of HCHO concentration, obtained by recording cyclically the background signal (without HCHO) and a signal from a HCHO standard. In Table 3 are summarized the performances of the different current on-line measurement techniques, only from the detection limit and response time points of view. A more extensive comparison is out of the scope of the present paper. This has been already done recently by Hak et al. (2005), Wisthaler et al. (2008) and Hottle et al. (2009), also including off-line techniques. Here we have considered the most recently developed techniques, so with on-line measurements, namely FTIR, Differential Optical Absorption Spectroscopy (DOAS), Laser Induced Fluorescence (LIF), fluorimetric Hantzsch reaction, and Proton-Transfer Reaction Mass Spectrometry. It is seen that the TDLAS technique offers the best compromise between sensitivity and time resolution, being only in real competition with LIF.

3.6 Selection of spectral lines in the 2600-3100 cm^{-1} band for HCHO stratospheric TDLAS measurements

The three TDLAS lines (2909.71, 2912.09 and 2914.46 cm^{-1}) studied in the present work may be used for in situ stratospheric measurements. These are among the most intense R-branch lines of the HCHO ν_5 band, compared to other lines in the 3.6 μm (2600-3100 cm^{-1}) spectral region. The feasibility of the measurements depends on the spectral interferences by other atmospheric species and on the detection limit of the instrument. Applied to the stratosphere, the detection limit derived in the laboratory measurements (in the above Section), that is 35 ppt HCHO for 280 m path length at 40 hPa and 294 K, reduces for instance to 6 ppt at about 16 km altitude and to 27 ppt at ~25 km, corresponding to typical pressures and temperatures of 110 hPa and 200 K and 25 hPa and 220 K, respectively, for the 431 m path length of SPIRALE balloon-borne instrument. These limits are well below the typical HCHO volume mixing ratios of 20 ppt and 50 ppt existing at the corresponding altitudes.

The selection of a suitable absorption line is critical for a species such as formaldehyde, which is a relatively weak absorber in the mid-infrared region and not very abundant in the stratosphere. In order to facilitate the HCHO retrievals from high-resolution measurements, it is necessary to select a strong and well-isolated absorption line to minimize as much as possible the impact of interfering species absorbing in the same spectral region. For this purpose, a simulation approach has been adopted to represent simultaneously the absorption

lines corresponding to most of stratospheric molecular species. Hence, a home-made program has been developed and was used to simulate interactively the transmission spectra of all the species included in the HITRAN 2008 database (Rothman et al., 2009) under a standard atmospheric condition defined by mid-latitude (45°) and time of the day (McClatchey et al., 1972; ESSA, NASA and U.S. Air Force, 1976). The operator has flexibility to change these parameters and other ones, such as the selected molecular species considered at a given altitude, the optical path length, and the spectral micro-window width. Line-by-line simulations have been performed over the whole 2600-3100 cm^{-1} domain, under a typical stratospheric condition, i.e. for 50 ppt HCHO at 25 km altitude. Figure 7 presents detailed parts of this band, with focus on the absorption lines of formaldehyde studied in this work. At 2909.71 cm^{-1} and 2914.46 cm^{-1} (Fig. 7, top and bottom), the HCHO lines are strongly hindered by those of O_3 and CH_4, respectively. It is clear that these lines cannot be used for the quantitative detection of this molecule in the stratosphere. At 2912.09 cm^{-1} (Fig. 7, middle), the formaldehyde line is partly perturbed by that of OCS located at 2912.106 cm^{-1}, but can be used taking into account this OCS line during the retrieval process.

Among all the HCHO lines in the 2600-3100 cm^{-1} region, we found that those located at 2809.83 and 2831.64 cm^{-1} are the most suited for the detection of this molecule, as illustrated in Fig. 8 (a) and (c), respectively. The latter has been used for long time by Fried et al. (2008, and references therein). These lines present the advantage to be relatively strong and are sufficiently isolated from those of other trace gases. Between the previous HITRAN database (Rothman et al., 2005) and the new one (Rothman et al., 2009, based on Perrin et al., 2009), the 2831.64-cm^{-1} line intensity value has been slightly corrected by an increase whereas the 2912.09-cm^{-1} line intensity has been decreased by a factor of ~2.5, which leads to about the same value for both lines (~$6.0\pm0.2 \times 10^{-20}$ cm $molecule^{-1}$), and therefore decrease the interest of using the later one studied for atmospheric measurements. Finally, it is to be noted that the HCHO absorption lines located at 2814.48 cm^{-1} and 2856.17 cm^{-1} are also clear of interfering species but about 20-30% lower than the most interesting ones quoted above, as shown in Fig. 8.

4 Conclusions

This study presents a validation of a tunable diode laser absorption spectrometer (TDLAS) for formaldehyde measurement by a FTIR spectrometer in an atmospheric

simulation chamber. As a first step, the FTIR HCHO spectrum, recorded in Euphore chamber and used as a reference in the present work, has been compared to most of other ones published. The both absorption integrated band intensities (1660-1820 and 2600-3100 cm^{-1}) have been revealed to be in agreement within 1% with the average of these previous ones, including the most recent study of Perrin et al. (2009), and also consistent each other as in the latter. Formaldehyde was generated *in situ* from the reaction of ethene with ozone. This well-documented reaction has been then investigated by FTIR and ozone UV-monitor, leading to a rate constant and a formaldehyde formation yield at 294 K that are in excellent agreement with the compiled literature data. The three ro-vibrational line intensities (at 2909.71, 2912.09 and 2914.46 cm^{-1}) used in the very high resolution TDLAS method were calibrated by FTIR spectra simultaneously recorded during ethene ozonolysis. The inferred values (Table 2) confirm those from the updated HITRAN database (Rothman et al., 2009), based on the study of Perrin et al. (2009) within 4-13%.

In addition, the TDLAS performances at low concentration of formaldehyde were assessed. A 2σ detection limit of 88 ppt volume mixing ratio with a response time of 60 s (or 340 ppt in 4 s) was obtained at 30 Torr and 294 K, for 112 m optical path, potentially leading to 35 ppt for 280 m. In comparison with the widespread conventional methods used in atmospheric simulation chamber studies, our TDLAS has been shown to be more sensitive than the on-line techniques (FTIR, DOAS, Hantzsch method, PTR-MS), and as much as sensitive as the dinitrophenylhydrazine (DNPH) derivatization followed by off-line high pressure liquid chromatography ultraviolet (HPLC-UV) analysis, but this one needing more than one hour sampling (Whistaler et al., 2008). Therefore, the TDLAS technical performances in terms of response time and detection limit are of great added value for laboratory applications, including mechanism and kinetics of chemical reactions. However, one should keep in mind that the number of species to be monitored and the accuracy of the monitoring are limited by the advances in the very high-resolution spectroscopic databases. The TDLAS implementation can thus be seen as a complementary analysis tool of chamber studies.

Concerning atmospheric embarked *in situ* measurements, formaldehyde quantification appears to be feasible in the stratosphere with TDLAS instrumentation such as SPIRALE balloon-borne spectrometer, using the 2912.09 cm^{-1} line with detection limits above few tens of ppt for 431 m optical path length. In the upper troposphere, the 2831.64 cm^{-1} line is a better choice since the OCS species is abundant and would hinder the 2912.09 cm^{-1} line. Another

interesting line, of similar intensity (> 5 × 10^{-20} cm $molecule^{-1}$) and clear of known spectroscopic interferences, is at 2809.83 cm^{-1}. Moreover, the 1660-1820 cm^{-1} band has to be considered as an alternative, with line intensities of the same order of magnitude. The use of the 1764.9 cm^{-1} line as in the work of Herndon et al. (2007) is an example for stratospheric measurements, but less convenient in the upper troposphere where H_2O lines interfere.

Acknowledgements

The authors thank the SPIRALE technical team (M. Chartier, L. Pomathiod, G. Chalumeau) for successful TDLAS operations in the ICARE atmospheric simulation chamber, and A. Perrin (LISA, CNRS-Université Paris 12) and D. Jacquemart (LADIR, CNRS-Université Paris 6) for fruitful discussions and making available the line intensity value measured at 2914.46 cm^{-1}. This work was financially supported by the European Commission through the 7th Framework Programme under the grant agreement #228335 (EUROCHAMP-2 Project) and by the French CNRS-INSU Programme National de Chimie Atmosphérique.

References

Anderson L G, Lanning J A, Barrell R, Miyagishima J, Jones R H, Wolfe P, 1996. Sources and sinks of formaldehyde and acetaldehyde: an analysis of Denver's ambient concentration data. *Atmospheric Environment*, 30: 2113–123.

Atkinson R, Baulch D L, Cox R A, Crowley J N, Hampson R F, Hynes R G, Jenkin M E, Rossi M J, Troe J, 2006. Evaluated kinetic and photochemical data for atmospheric chemistry: Volume II – gas phase reactions of organic species. *Atmospheric Chemistry and Physics*, 6: 3625–4055.

Barth M C, Kim S W, Skamarock W C, Stuart A L, Pickering K E, Ott L E, 2007. Simulations of the redistribution of formaldehyde, formic acid, and peroxides in the 10 July 1996 Stratospheric-Tropospheric Experiment: Radiation, Aerosols, and Ozone deep convection storm, *Journal of Geophysical Research*, 112: D13310. DOI: 10.1029/2006JD008046.

Berthet G, Huret N, Lefèvre F, Moreau G, Robert C, Chartier M, Catoire V, Barret B, Pisso I, Pomathiod L, 2006. On the ability of chemical transport models to simulate the vertical structure of the N_2O, NO_2 and HNO_3 species in the mid-latitude stratosphere. *Atmospheric Chemistry and Physics*, 6: 1599–1609.

Berthet G, Renard J B, Catoire V, Chartier M, Robert C, Huret N, Coquelet F, Bourgeois Q, Rivière E D, Barret B, Lefèvre F, Hauchecorne A, 2007. Remote sensing measurements in the polar vortex: comparison to in situ observations and implications for the simultaneous retrievals and analysis of the NO_2 and OClO species. *Journal of Geophysical Research*, 112: D21310, doi:10.1029/2007JD008699.

Brauers T, Bossmeyer J, Dorn H P, Schlosser E, Tillmann R, Wegener R, Wahner A, 2007. Investigation of the formaldehyde differential absorption cross section at high and low spectral resolution in the simulation chamber SAPHIR. *Atmospheric Chemistry and Physics*, 7: 3579–3586.

Carlier P, Hannachi H, Mouvier G, 1986. The chemistry of carbonyl compounds in the atmosphere – a review. *Atmospheric Environment*, 20: 2079–2099.

Coheur P F, Herbin H, Clerbaux C, Hurtmans D, Wespes C, Carleer M, Turquety S, Rinsland C P, Remedios J, Hauglustaine D, Boone C D, Bernath P F, 2007. ACE-FTS observation of a young biomass burning plume: first reported measurements of C_2H_4, C_3H_6O, H_2CO and PAN by infrared occultation from space. *Atmospheric Chemistry and Physics*, 7: 5437–5446.

Cortesi U, Lambert J C, De Clercq C, Bianchini G, Blumenstock T, Bracher A, Castelli E, Catoire V, Chance K V, De Mazière M, Demoulin P, Godin-Beekmann S, Jones N, Jucks K. Keim C, Kerzenmacher T, Kuellmann H, Kuttippurath J, Iarlori M, Liu G Y, Liu Y, McDermid I S, Meijer Y J, Mencaraglia F, Mikuteit S, Oelhaf H, Piccolo C, Pirre M, et al., 2007. Geophysical validation of MIPAS-ENVISAT operational ozone data. *Atmospheric Chemistry and Physics*, 7: 4807–4867.

Crawford J, Davis D, Olson J, Chen G, Liu S, Gregory G, Barrick J, Sachse G, Sandholm S, Heikes B, Singh H, Blake D, 1999. Assessment of upper tropospheric HO_x sources over the tropical Pacific based on NASA GTE/PEM data: Net effect on HO_x and other photochemical parameters, *Journal of Geophysical Research*, 104(D13): 16255. DOI: 10.1029/1999JD900106.

Dufour G, Szopa S, Barkley M P, Boone C D, Perrin A, Palmer P I, Bernath P F, 2009. Global upper-tropospheric formaldehyde: seasonal cycles observed by the ACE-FTS satellite instrument. *Atmospheric Chemistry and Physics*, 9: 3893–3910.

ESSA, NASA, U.S. Air Force, 1976. U.S. Standard Atmosphere 1976 and Supplements 1966. *U.S. Government Printing Office*, Washington D C, U.S.A.

EUPHORE FTIR References Database, (available online at http://euphore.es/FTIRReferences/index.htm).

Fenske J D, Hasson A S, Paulsen S E, Kuwata K T, Ho A, Houk K N, 2000. The pressure dependence of the OH radical yield from ozone-alkene reactions. *Journal of Physical Chemistry A*, 104: 7821–7833.

Fried A, Walega J G, Olson J R, Crawford J H, Chen G, Weibring P, Richter D, Roller C, Tittel F K, Heikes B G, Snow J A, Shen H, O'Sullivan D W, Porter M, Fuelberg H, Halland J, Millet D B, 2008. Formaldehyde over North America and the North Atlantic during the summer 2004 INTEX campaign: Methods, observed distributions, and measurement-model comparisons. *Journal of Geophysical Research*, 113: D10302, doi:10.1029/2007JD009185.

Gratien A, Picquet-Varrault B, Orphal J, Perraudin E, Doussin J F, Flaud J M, 2007. Laboratory intercomparison of the formaldehyde absorption cross sections in the infrared (1600–1820 cm^{-1}) and ultraviolet (300–360 nm) spectral regions. *Journal of Geophysical Research*, 112: D05305, doi:10.1029/2006JD007201.

Hak C, Pundt I, Trick S, Kern C, Platt U, Dommen J, Ordóñez C, Prévôt A S H, Junkermann W, Astorga-Lloréns C B, Larsen R, Mellqvist J, Strandberg A, Yu Y, Galle B, Kleffmann J, Lörzer J C, Braathen G O, Volkamer R, 2005. Intercomparison of four different in-situ techniques for ambient formaldehyde measurements in urban air. *Atmospheric Chemistry and Physics*, 5: 2881–2900.

Heikes B G, 1992. Formaldehyde and hydroperoxides at Mauna Loa Observatory. *Journal of Geophysical Research*, 97(D16): 18001–18013.

Herndon S C, Nelson Jr D D, Yongquan L, Zahniser M S, 2005. Determination of line strengths for selected transitions in the ν_3 relative to the ν_1, and ν_5 bands of H_2CO. *Journal of Quantitative Spectroscopy & Radiative Transfer*, 90: 207–216.

Herndon S C, Zahniser M S, Nelson Jr D D, Shorter J, McManus J B, Jiménez R., Warneke C., de Gouw J A, 2007. Airborne measurements of HCHO and HCOOH during the New England Air Quality Study 2004 using a pulsed quantum cascade laser spectrometer. *Journal of Geophysical Research*, 112: D10S03, doi:10.1029/2006JD007600.

Horie O, Moortgat G K, 1998. The effect of the addition of CO on the reaction of ozone with ethane. *Chemical Physics Letters*, 288: 464–472.

Hottle J R, Huisman A J, Digangi J P, Kammrath A, Galloway M M, Coens K L, Keutsch F N, 2009. A laser induced fluorescence-based instrument for in situ measurements of atmospheric formaldehyde. *Environmental Science and Technology*, 43: 790–795.

Huret N, Pirre M, Hauchecorne A, Robert C, Catoire V, 2006. On the vertical structure of the stratosphere at midlatitudes during the first stage of the polar vortex formation and in the polar region in the presence of a large mesospheric descent. *Journal of Geophysical Research*, 111: D06111, doi:10.1029/2005JD006102.

Jacquemart D, 2009. *Personal communication*.

Jégou F, Urban J, de La Noë J, Ricaud P, Le Flochmoën E, Murtagh D P, Eriksson P, Jones A, Petelina S, Llewellyn E J, Lloyd N D, Haley C, Lumpe J, Randall C, Bevilacqua R M, Catoire V, Huret N, Berthet G, Renard J B, Strong K, Davies J, Mc Elroy C T, Goutail F, Pommereau J P, 2008. Technical Note: Validation of Odin/SMR limb observations of ozone, comparisons with OSIRIS, POAM III, ground-based and balloon-borne instruments. *Atmospheric Chemistry and Physics*, 8: 3385–3409.

Jobson B T, McCoskey J K, 2010. Sample drying to improve HCHO measurements by PTR-MS instruments: laboratory and field measurements. *Atmospheric Chemistry and Physics*, 10: 1821–1835.

Joly L, Robert C, Parvitte B, Catoire V, Durry G, Richard G, Nicoullaud B, Zéninari V, 2008. Development of a spectrometer using a cw DFB quantum cascade laser operating at room temperature for the simultaneous analysis of N_2O and CH_4 in the Earth's atmosphere. *Applied Optics*, 47: 1206–1214.

Klotz B, Barnes I, Imamura T, 2004. Product study of the gas-phase reactions of O_3, OH and NO_3 radicals with methyl vinyl ether. *Physical Chemistry Chemical Physics*, 6, 1725–1734.

Kroll J H, Clarke J S, Donahue N M, Anderson J G, Demerjian K L, 2001. Mechanism of HO_X formation in the gas-phase ozone-alkene reaction. 1. Direct, pressure-dependent measurements of prompt OH yields. *Journal of Physical Chemistry A*, 105: 1554–1560.

Lee Y N, Zhou X, Kleinman L I, Nunnermacker L J, Springston S R, Daum P H, Newman L, Keigley W G, Holdren M W, Spicer C W, Young V, Fu B, Parrish D D, Holloway J, Williams J, Roberts J M, Ryerson T B, Fehsenfeld F C, 1998. Atmospheric chemistry and distribution of formaldehyde and several multioxygenated carbonyl compounds during the 1995 Nashville/Middle Tennessee Ozone Study. *Journal of Geophysical Research*, 103(D17): 22449–22462.

Lelieveld J, Crutzen P J, 1990. Influences of cloud photochemical processes on tropospheric ozone. *Nature*, 343: 227–233, doi:10.1038/343227a0.

McClatchey R, Fenn R, Selby J, Volz F, Garing J, 1972. Optical properties of the atmosphere, 3rd ed., AFCRL-TR-72-0497. *Environmental Research Paper*, 411.

Mébarki Y, Catoire V, Huret N, Berthet G, Robert C, Poulet, G, 2010. More evidence for very short-lived substance contribution to stratospheric chlorine inferred from HCl balloon-borne in situ measurements in the tropics. *Atmospheric Chemistry and Physics*, 10: 1–13.

Mihelcic D M, Heitlinger M D, Kley D, Müsgen P, Volz-Thomas A, 1999. Formation of hydroxyl and hydroperoxy radicals in the gas-phase ozonolysis of ethane. *Chemical Physics Letters*, 301: 559–564.

Moreau G, Robert C, Catoire V, Chartier M, Camy-Peyret C, Huret N, Pirre M, Pomathiod L, Chalumeau G, 2005. SPIRALE: a multispecies in situ balloon-borne instrument with six tunable diode laser spectrometers. *Applied Optics*, 44(28), 5972–5989.

Müller R, Tilmes S, Grooß J U, Engel A, Oelhalf H, Wetzel G, Huret N, Pirre M, Catoire V, Toon G, Nakajima H, 2007. Impact of mesospheric intrusions on ozone-tracer relations in the stratospheric polar vortex. *Journal of Geophysical Research*, 112: D23307, doi:10.1029/2006JD008315.

Nakanaga T, Kondo S, Saëki, S, 1982. Infrared band intensities of formaldehyde and formaldehyde-D2. *Journal of Chemical Physics*, 76: 3860–3865.

Neeb P, Horie O, Moortgat G K, 1998. The ethene–ozone reaction in the gas phase. *Journal of Physical Chemistry A*, 102: 6778–6785.

Paulson S E, Fenske J D D, Sen A D, Callahan T W, 1999. A novel small-ratio relative-rate technique for measuring OH formation yields from the reactions of O_3 with alkenes in the gas phase, and its application to the reactions of ethene and propene. *Journal of Physical Chemistry A*, 103: 2050–2059.

Perrin A, Valentin A, Daumont L, 2006. New analysis of the ν_1, ν_5, $2\nu_4$, $\nu_4+\nu_6$, $2\nu_6$, $\nu_3+\nu_4$, $\nu_3+\nu_6$, $\nu_2+\nu_4$, $2\nu_3$, $\nu_2+\nu_6$, and $\nu_2+\nu_3$ bands of formaldehyde H_2CO: Line positions and intensities in the 3.6 μm spectral region. *Journal of Molecular Structure*, 780: 28–44.

Perrin A, Jacquemart D, KwabiaTchana F, Lacome N, 2009. Absolute line intensities measurements and calculations for the 5.7 and 3.6 μm bands of formaldehyde. *Journal of Quantitative Spectroscopy & Radiative Transfer*, 110(9-10): 700–716.

Pirre M, Pisso I, Marécal V, Catoire V, Mébarki Y, Robert C, 2008. Intrusion of recent air in midlatitude stratosphere revealed by in situ tracer measurements and trajectory calculations. *Journal of Geophysical Research*, 113: D11302, doi: 10.1029/2007JD009188.

Possanzini M, Di Palo V, Cecinato A, 2002. Sources and photodecomposition of formaldehyde and acetaldehyde in Rome ambient air. *Atmospheric Environment*, 36: 3195–3201.

Ricaud P, Alexandre D, Barret B, Le Flochmoën E, Motte E, Berthet G, Lefèvre F, Murtagh D, 2007. Measurements of mid-stratospheric formaldehyde from the Odin/SMR instrument. *Journal of Quantitative Spectroscopy & Radiative Transfer*, 107: 91–104.

Renard J B, Berthet G, Brogniez C, Catoire V, Fussen D, Goutail F, Oelhaf H, Pommereau J P, Roscoe H K, Wetzel G, Chartier M, Robert C, Balois J Y, Verwaerde C, Auriol F, François P, Gaubicher B, Wursteisen P, 2008. Validation of GOMOS-Envisat vertical profiles of O_3, NO_2, NO_3, and aerosol extinction using balloon-borne instruments and analysis of the retrievals. *Journal of Geophysical Research*, 113: A02302, doi:10.1029/2007JA012345.

Rickard A R, Johnson D, McGill C D, Marston G, 1999. OH yields in the gas-phase reactions of ozone with alkenes. *Journal of Physical Chemistry A*, 103: 7656–7664.

Robert C, 2007. Simple, stable, and compact multiple-reflection optical cell for very long optical paths. *Applied Optics*, 46(22): 5408–5418.

Rothman L S, Jacquemart D, Barbe A, Chris Bennerc D, Birk M, Brown L R, Carleer M R, Chackerian Jr C, Chance K, Coudert L H, Dana V, Devi V M, Flaud J M, Gamache R R,

Goldman A, Hartmann J M, Jucks KW, Maki A G, Mandin J Y, Massie S T, Orphal J, Perrin A, Rinsland C P, Smith M A H, Tennyson J, Tolchenov R N, Toth R A, Vander Auwera J, Varanasi P, Wagner G, 2005. The HITRAN 2004 molecular spectroscopic database. *Journal of Quantitative Spectroscopy & Radiative Transfer*, 96: 139–204.

Rothman L S, Gordon I E, Barbe A, Chris Bennerc D, Bernath P F, Birk M, Boudon V, Brown L R, Campargue A, Champion J P, Chance K, Coudert L H, Dana V, Devi V M, Fally S, Flaud J M, Gamache R R, Goldman A, Jacquemart D, Kleiner I, Lacome N, Lafferty W J, Mandin J Y, Massie S T, Mikhailenko S N, Miller C E, Moazzen-Ahmadi N, Naumenko O V, Nikitin A V, Orphal J, Perevalov V I, Perrin A, Predoi-Cross A, Rinsland C P, Rotger M, Simeckova M, Smith M A H, Sung K, Tashkun S A, Tennyson J, Toth R A, Vandaele A C, Vander Auwera J, 2009. The HITRAN 2008 molecular spectroscopic database. *Journal of Quantitative Spectroscopy & Radiative Transfer*, 110: 533–572.

Seinfeld J H, Pandis S N, 2006. Atmospheric Chemistry and Physics, 2nd Edition, J Wiley & Sons, Inc, Hoboken, New Jersey (U.S.A.).

Sharpe S W, Johnson T J, Sams R L, Chu P M, Rhoderick G C, Johnson P A, 2004. Gas-phase databases for quantitative infrared spectroscopy. *Applied Spectroscopy*, 58: 1452--1461.

Steck T, Glatthor N, von Clarmann T, Fischer H, Flaud J M, Funke B, Grabowski U, Höpfner M, Kellmann S, Linden A, Perrin A, Stiller G P, 2008. Retrieval of global upper tropospheric and stratospheric formaldehyde (H_2CO) distributions from high-resolution MIPAS-Envisat spectra. *Atmospheric Chemistry and Physics*, 8: 463–470.

Strong K, Wolff M A, Kerzenmacher T E, Walker K A, Bernath P F, Blumenstock T, Boone C, Catoire V et al., 2008. Validation of ACE-FTS N_2O measurements. *Atmospheric Chemistry and Physics*, 8: 4759–4786.

Tie X, Brasseur G, Emmons L, Horowitz L, Kinnison D, 2001. Effects of Aerosols on Tropospheric Oxidants: A Global Model Study. *Journal of Geophysical Research*, 106(D19): 22931–22964.

Wang D Y, Hopfner M, Blom C E, Ward W E, Fischer H, Blumenstock T, Hase F, Keim C, Liu G Y, Mikuteit S, Oelhaf H, Wetzel G, Cortesi U, Mencaraglia F, Bianchini G, Redaelli G, Pirre M, Catoire V, Huret N et al., 2007. Validation of MIPAS HNO_3 operational data. *Atmospheric Chemistry and Physics*, 7: 4905–4934.

Wert B P, Fried A, Henry B, Cartier S, 2002. Evaluation of inlets used for the airborne measurement of formaldehyde. *Journal of Geophysical Research*, 107(D13): 4163, doi:10.1029/2001JD001072.

Wegener R, Brauers T, Koppmann R, Rodríguez Bares S, Rohrer F, Tillmann R, Wahner A Hansel A, Wisthaler A, 2007. Simulation chamber investigation of the reactions of ozone with short-chained alkenes. *Journal of Geophysical Research*, 112(D13301): doi:10.1029/2006JD007531.

Wisthaler A E, Apel C, Bossmeyer J, Hansel A, Junkermann W, Koppmann R, Meier R, Müller K, Solomon S J, Steinbrecher R, Tillmann R, Brauers T, 2008. Technical Note: Intercomparison of formaldehyde measurements at the atmosphere simulation chamber SAPHIR. *Atmospheric Chemistry and Physics*, 8: 2189–2200.

Table 1. Comparison of the calculated Integrated Band Intensities (IBIs) in the regions 1660-1820 cm^{-1} and 2600-3100 cm^{-1} using different IR spectra (T = 296±2 K).

Wavenumber (cm^{-1})	IBI × 10^{17} (cm $molecule^{-1}$)	Resolution (cm^{-1})	Method	Reference
1660-1820	1.229 ± 0.040	0.25	FTIR	Nakanaga et al., 1982
	1.248 ± 0.126	1	FTIR	Klotz et al., 2004
	1.262 ± 0.083	~10^{-3}	TDLAS	Herndon et al., 2005
	1.284 ± 0.064	0.11	FTIR	Sharpe et al., 2004
	1.31 ± 0.04	0.08	FTIR/UV	Gratien et al., 2007
	1.242 ± 0.087	0.0035	FTIR	Perrin et al., 2009
	1.265 ± 0.063	1	FTIR	Euphore
2600-3100	2.708 ± 0.099	0.25	FTIR	Nakanaga et al., 1982
	2.800 ± 0.140	0.1	FTIR	Sharpe et al., 2004
	2.92 ± 0.10	0.08	FTIR/UV	Gratien et al., 2007
	2.79 ± 0.25	0.0035	FTIR	Perrin et al., 2009
	2.830 ± 0.141	1	FTIR	Euphore

Table 2. Ro-vibrational line intensities determined in this work and comparison with previous studies

Wavenumber (cm^{-1})	Global line intensity S [a]	Reference
2909.71	6.6 ± 0.7	This work
	5.78 ± 0.41	Perrin et al. (2009) [b]
	10.24 [c]	Rothmann et al. (2005) [d]
2912.09	6.0 ± 0.6	This work
	6.22 ± 0.44	Perrin et al. (2009) [e]
	15.12 [c]	Rothman et al. (2005) [f]
2914.46	6.1 ± 0.6	This work
	5.9 ± 0.3	Jacquemart et al. (2009) [g]
	5.57 ± 0.39	Perrin et al. (2009) [h]
	9.20 [c]	Rothman et al. (2005) [i]

[a] units of 10^{-20} cm molecule^{-1}; Reported uncertainties are overall, including precision (1σ) and estimated systematic errors. [b] Sum of two equal intensity lines at 2909.71338 and 2909.71353 cm^{-1}. [c] Unknown uncertainty according to the author. [d] Sum of two equal intensity lines at 2909.71300 cm^{-1}. [e] Sum of four intensity lines: two of equal intensities (2.84) at 2912.09179 and 2912.09198 cm^{-1}, and two of equal intensities (0.27) at 2912.10063 and 2912.10132 cm^{-1}. [f] Sum of three equal intensity lines at 2912.09180 cm^{-1}. [g] Experimental value obtained by Jacquemart et al. (2009) in the study of Perrin et al. (2009). [h] Sum of two equal intensity (2.771) lines at 2914.45917 and 2914.46110 cm^{-1} and one intensity line (0.031) at 2914.46962 cm^{-1}. [i] Sum of two equal intensity lines at 2914.45980 cm^{-1}.

Table 3. Comparison of TDLAS with other on-line techniques

Instrumentation (Reference)	2σ detection limit [a] (optical path length)	Accuracy (%)	Typical time resolution
TDLAS (This work)	340 ppt (112.3 m) 88 ppt (112.3 m) 35 ppt (280 m)	10	4 s 60 s 60 s
TDLAS (Fried et al., 2008)	360 ppt (100 m) 66 ppt (100 m)	13	1 s 60 s
FTIR (This work; Hak et al., 2005)	400 (1000 m) 4800 ppt (166 m)	6-27	5 min 4 min
DOAS [b] (Wisthaler et al., 2008)	400 ppt	6	100 s
LIF [c] (Hottle et al., 2009)	34 ppt 6.2 ppt	25	1 s 30 s
Fluorimetric Hantzsch reaction (Wisthaler et al., 2008)	50 – 80 ppt	5-8	1 – 2 min
PTR-MS [d] (Wisthaler et al., 2008; Jobson et al., 2010)	80 – 200 ppt	10-15	75 s

[a] The 1σ precision can be derived as the half of this detection limit. [b] Differential Optical Absorption Spectroscopy. [c] Laser Induced Fluorescence. [d] Proton-Transfer Reaction Mass Spectrometry.

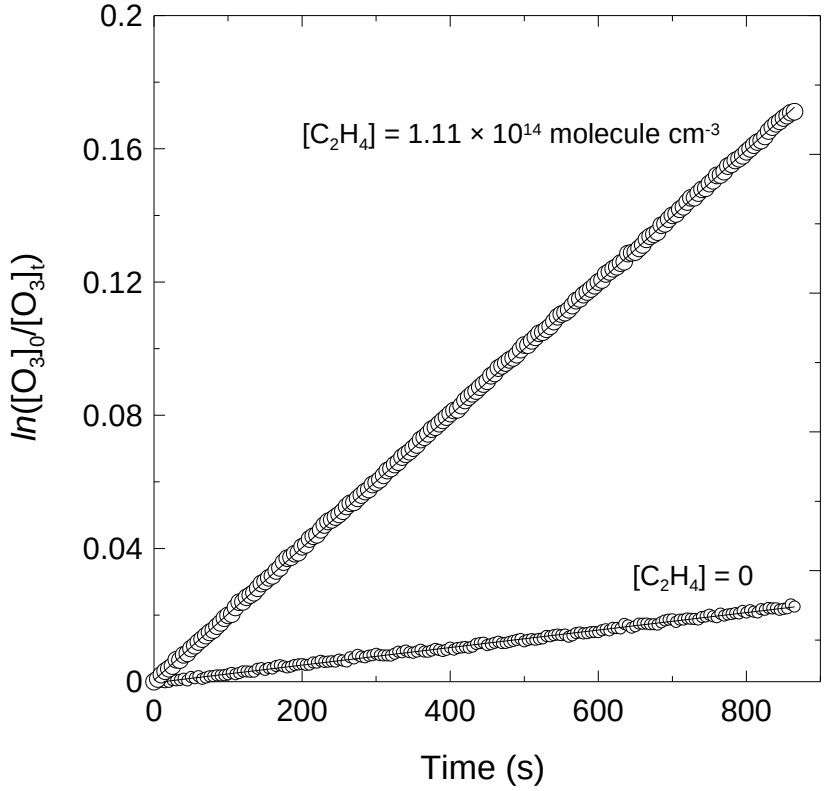

Fig. 1. Ozone loss in the absence and presence of 4.5 ppm C_2H_4 (i.e. 1.11×10^{14} molecules cm^{-3}).

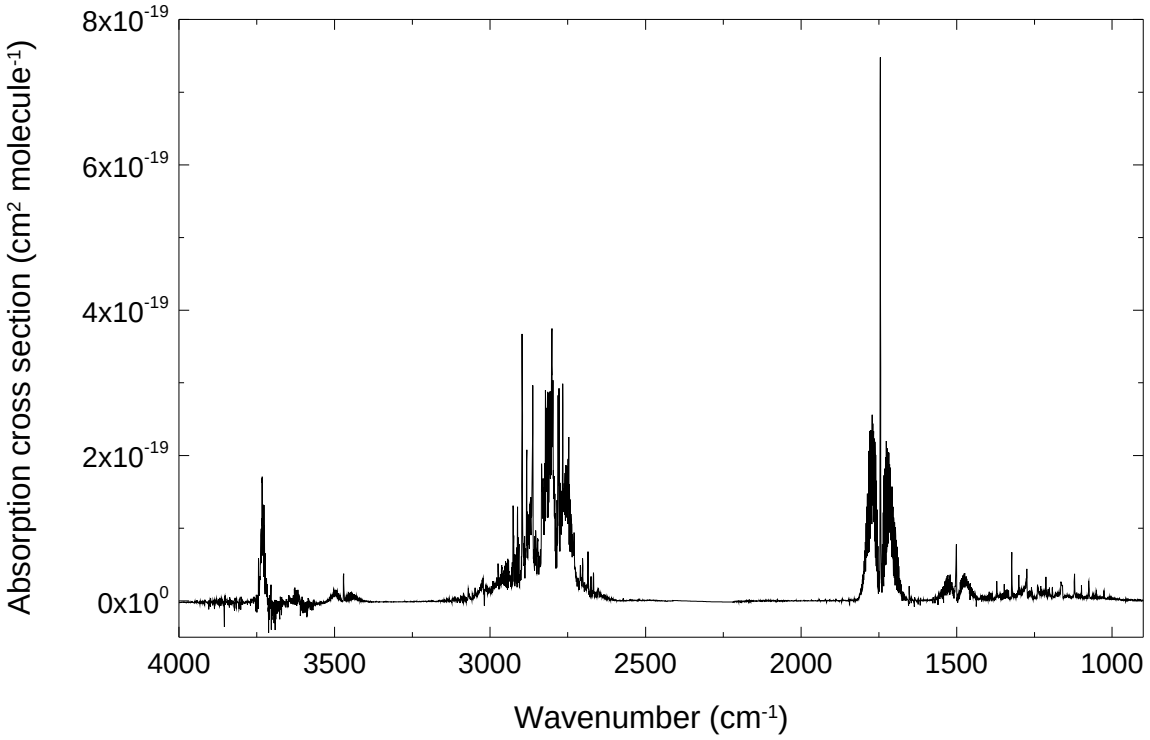

Fig. 2. Reference spectrum of 892.4 ppb formaldehyde at T = 296.5°C and P = 1004.5 mbar recorded at Euphore at a resolution of 1 cm^{-1}.

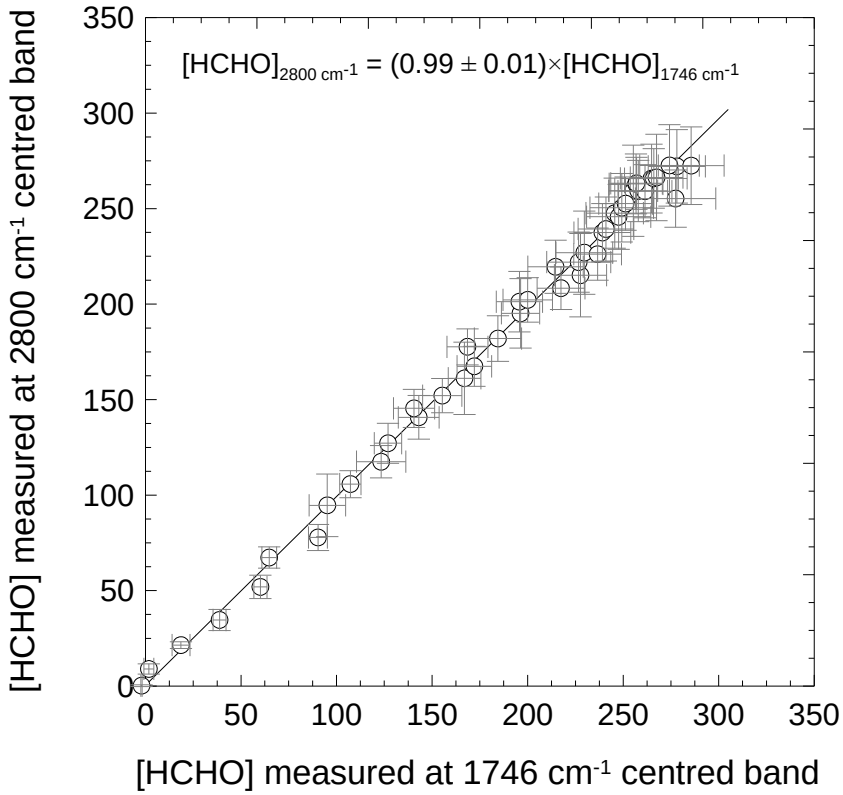

Fig. 3. Correlation between measurements performed with the 1660-1820 cm^{-1} band (centred at 1746 cm^{-1}) and the 2600-3100 cm^{-1} band (centred at 2800 cm^{-1})

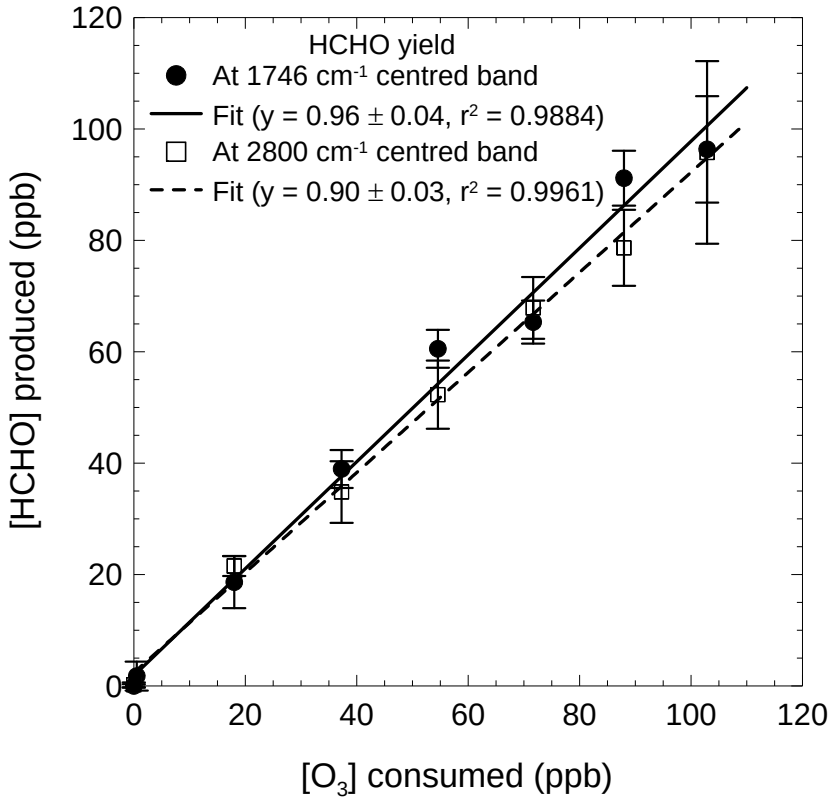

Fig. 4. HCHO formation yield from ozonolysis of ethene obtained from the 1746 cm^{-1} and 2800 cm^{-1} centred bands at early stage of the reaction.

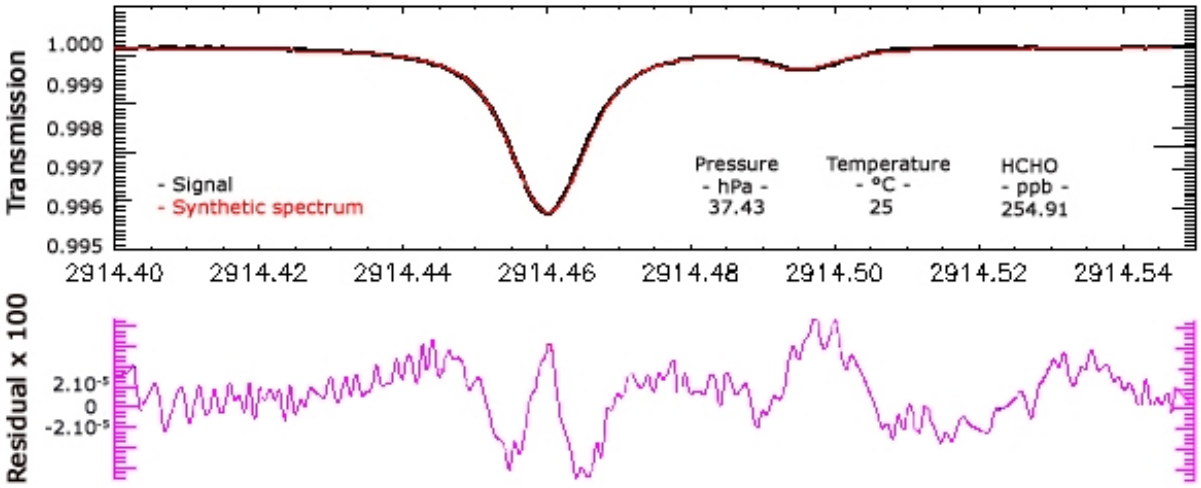

Fig. 5. Example of a spectral micro-window used to retrieve the HCHO line intensity *S* at 2914.46 cm^{-1} by TDLAS. Top: The black line represents the experimental transmission spectrum and the red line the synthetic transmission spectrum. Bottom: The pink line represents the residual of the signal, i.e. the subtraction between the experimental and synthetic signals. Statistical precision on this fit is 1.5% (1σ).

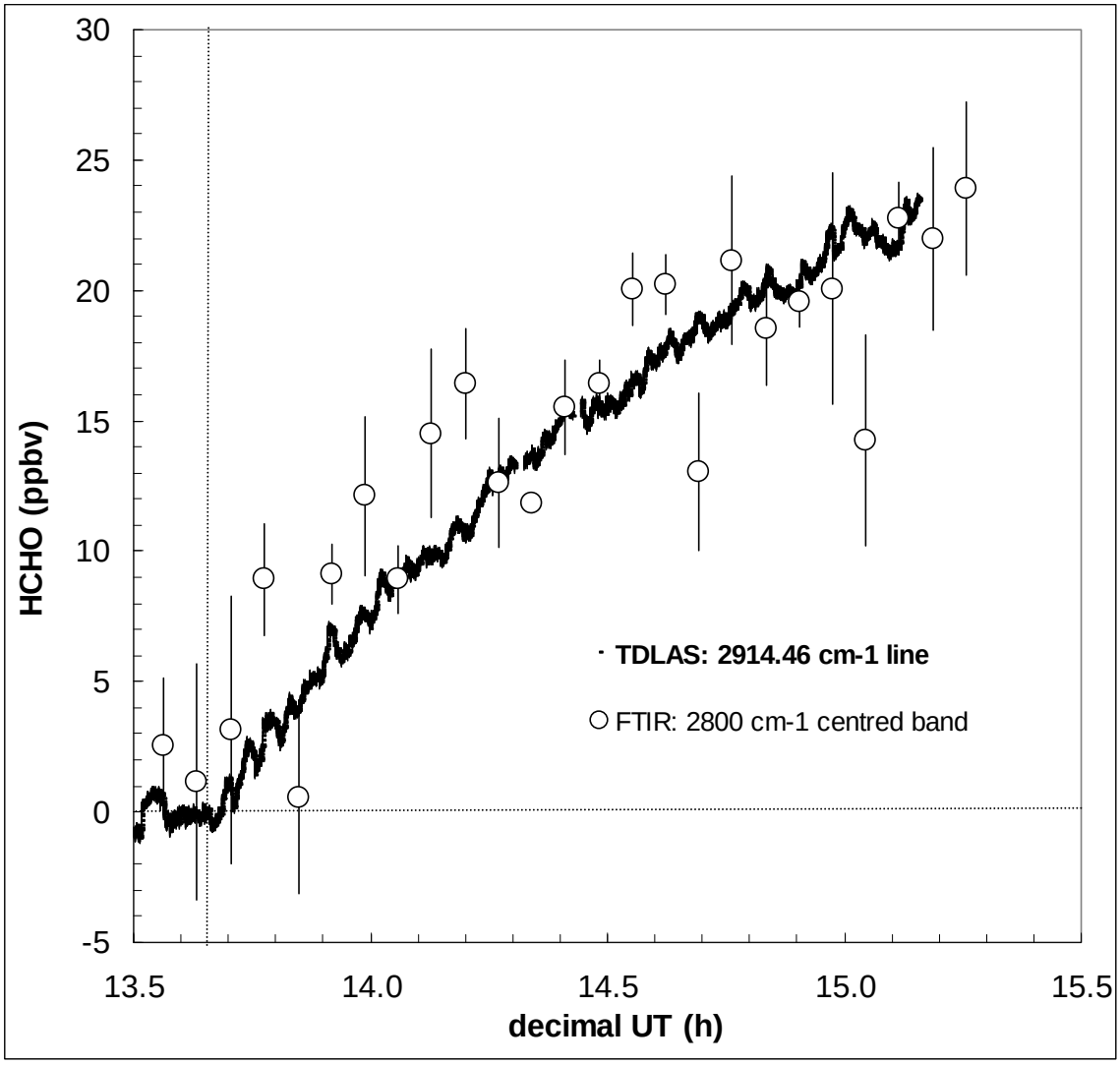

Fig. 6. Concentration time-profiles of formaldehyde using TDLAS and FTIR measurements during ethene ozonolysis reaction, with initial volume mixing ratios of 219.0±0.1 ppb O_3 and 681±30 ppb C_2H_4. Error bars are labelled for each measurement point and represent only 1σ precision. The horizontal and vertical dotted lines represent the zero HCHO concentration and the reactant mixing beginning (13.66 h), respectively.

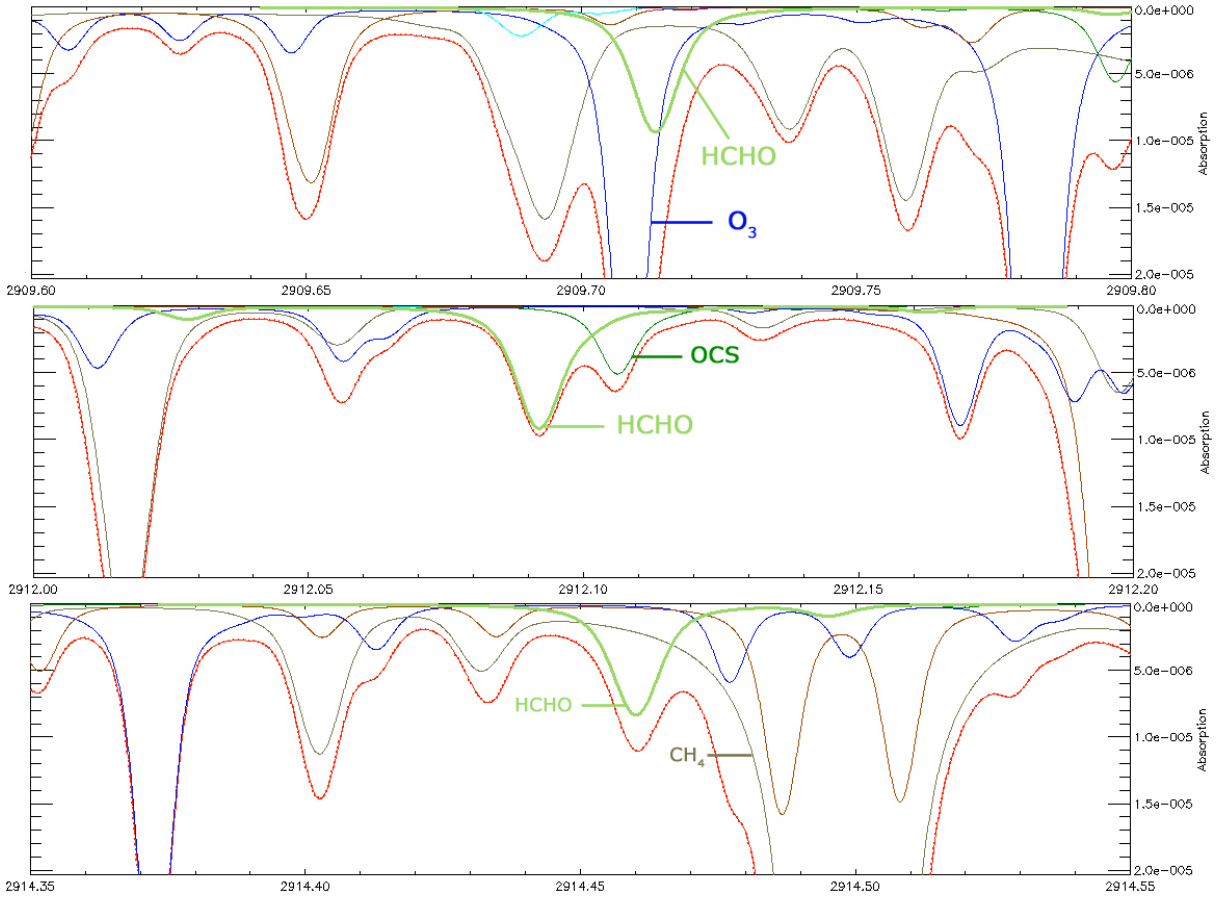

Fig. 7. Simulations of the transmission spectra at 25 km altitude, around 2909.71 cm^{-1} (top), 2912.09 cm^{-1} (middle) and 2914.46 cm^{-1} (bottom), considering a 431 m optical path (SPIRALE configuration) and based on HITRAN 2008 spectroscopic parameters (Rothman et al., 2009). The transmission spectra are color-coded (green: HCHO, blue: O_3, dark green: OCS, grey: CH_4; brown: NO_2, turquoise: H_2O) for each species and the red line indicates the total transmission.

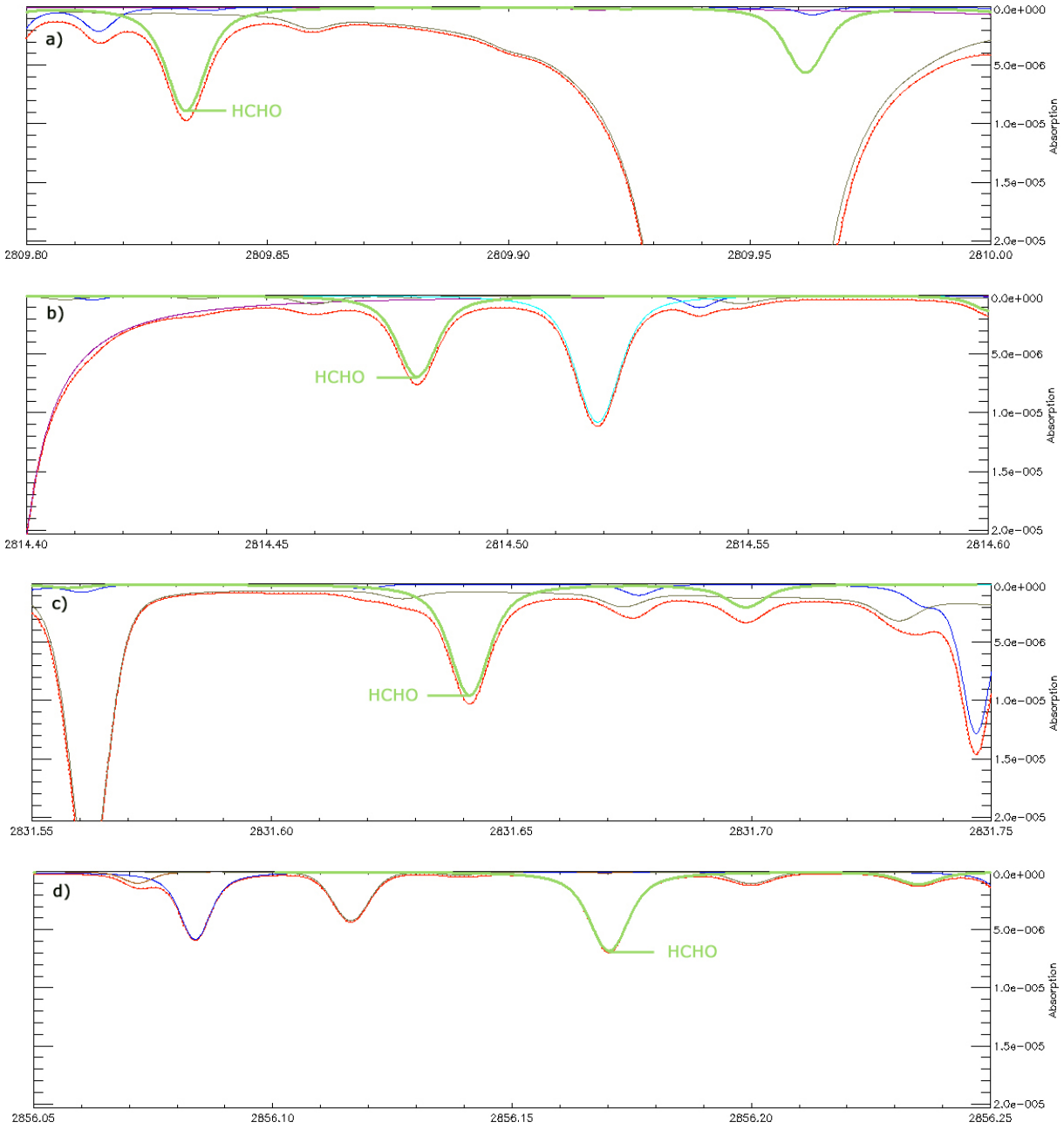

Fig. 8. Simulations of transmission spectra at 25 km altitude around: (a) 2809.83 cm^{-1}, (b) 2814.48 cm^{-1}, (c) 2831.64 cm^{-1}, (d) 2856.17 cm^{-1}, considering a 431m optical path (SPIRALE configuration) and based on HITRAN 2008 spectroscopic parameters (Rothman et al., 2009). The transmission spectra are color-coded for each species (see Fig. 7 caption for detail) and the red line indicates the total transmission.